Strain-Energy Criterion based Method of Numerical Simulation for Trabecular Bone Remodeling — (I) Bone Fracture Healing*

Bingzhi Chen, Yuanxian Gu, Zhan Kang, Shutian Liu

State Key Laboratory of Structural Analysis for Industrial Equipment,
Dept. of Engineering Mechanics, Dalian University of Technology, Dalian 116024, China

Abstract. Combined with the finite element and the structural optimization methods, one remodeling model of bone fracture healing is proposed on the basis of the strain-energy density criterion. The strain-energy density is taken as the mechanical stimulus of bone remodeling, and the fracture healing is presented as internal remodeling of trabecular bones and described with the change of material density distribution. The numerical results demonstrate that the proposed method can effectively simulate the process of bone fracture healing and illuminate the mechanism of healing processing of bone fracture as well.

Keywords: bone remodeling; fracture healing; strain-energy density; resorption; formation; osteotylus;

1. Introduction

The bone remodeling is one of interesting topics of biomechanics. In this field, the Wolff's law widely accepted and supported by experiments has shown that the principal stress directions indeed align with trabecular bone sites (Biewener et al., 1996; Hayes an Snyder, 1981). Firoozbakhsh and Cowin (1980) investigated the remodeling behavior of an initially inhomogeneous, orthotropic cylinder subjected to a period axial compressive load. More recent studies on adult animals in vivo (Chow et al., 1993) have shown a dose-response relationship between the applied loads and the formation rate of trabecular bones, and suggested that the shape and thickness of individual trabecular are modeled by loads. Fyhrie and Schaffler (1995) used the method of strain tolerate error which led to trabecular remodeling to study the relationship between strain and apparent density of trabecular bones. Charels et al (1997) and Christopher et al (1997) discussed the relationship between density distribution and modeling stimulus. Bone maintenance theory has also been developed these years. Stipner (1995), Huiskes (1992) and Poss et al (1988) considered the two-dimensional model of femur and studied the remodeling phenomenon of stress accumulation.

This paper is aimed at to combine the research in bone mechanics and computational structural mechanics. On the basis of the structural optimization theory and the finite element analysis method, one numerical simulation method to predict bone remodeling is proposed. Utilizing the adaptive elasticity theory of bone remodeling, taking element material density as design variable, we form the optimization model of bone material density distribution. The optimization distribution of bone material is the result of bone remodeling. To solve this optimization problem, the optimality criteria method and sequence linear programming method are adopted here. An optimization algorithm based on the strain energy density criterion is proposed to solve the inverse problem of numerical simulation of the internal remodeling of trabecular bones. The computation is implemented in the software JIFEX developed for the structural finite element analysis and design optimization. As example, healing process of bone fracture is simulated here. It is shown that the numerical simulation provode results which are in accordance with the actual situation.

2. Numerical Method of Remodeling Simulation

On the basis of the adaptive elasticity theory (Cowin et al.1976) and strain energy criterion (Charles et al.1997), bone remodeling model is proposed. It is combined with bone optimization equations and finite element method to solve the problem of bone remodeling. The fracture healing process of bone is simulated and the mechanism of the fracture healing process is discussed.

2.1 Governing equation of the reference strain-energy criterion

The finite element stress analysis is used to calculate stresses and strains within the bone. The strain energy, denoted as U, can be expressed by the stresses and strains as

$$U = \frac{1}{2}\{\sigma\}\{\varepsilon\} \tag{1}$$

* The project supported by the Scientific Fund for National Outstanding Youth of China (19525206) and the NKBRSF of China (No. G1999032805).

From these mechanical variables, a stimulus is determined, which controls the rate of bone remodeling. The relation between the strain energy stimulus and the rate of change of bone density can be described in a remodeling governing rule. The actual bone density is then related to the modulus of elasticity of the bone, hence an updated input for the FEM model. The iterative procedure stops when the objective is reached or when the bone density has reached its maximum or minimal value. So the remodeling governing equation is stated as:

$$\frac{1}{n}\sum_{i=1}^{n}\frac{U_i}{\rho}=\frac{U_a}{\rho} \tag{2}$$

$$\Delta\rho = B\left(\frac{U_a}{\rho}-k\right) \tag{3}$$

where U_i (MPa) is the strain energy density (SED) for loading case i, as calculated in a continuum model of the bone material. Ua is the average SED over all n loading cases, ρ (g/cm^3) is the apparent density and $\Delta\rho$ is a change of density, k is a constant called reference stimulus, B is the remodeling coefficient, which is time dependent. Eq.(3) is the bone remodeling governing equation of the strain-energy criterion.

The value of k is fixed in the specific period and human. The quantity Ua/ ρ (Joules/gram) represents the remodeling stimulus and is assumed to be sensed by bone specimen cells. It depends on the quantity Ua/ ρ to determine whether bone formulation or resorption is taken for the case that place. When Ua/ρ-k≠0, there is a driving force which led to bone formation or resorption. When the driving force is negative, bone resorption occurs, while the driving force is positive, the force will induce bone formation. However, that is not so simple in practice. When driving force U_a/ρexceed or lower than the reference stimulus k in a less range, the bone remodeling will not occur, which is called dead zone. Bone remodeling will not be induced if there exists a small difference between the actual strain energy density and reference strain-energy density k. Hence, there always exists one specific dead zone s. Eq.(3) can be described as following

$$\frac{d\rho}{dt}=B\left\{\frac{U_a}{\rho}-k(1+s)\right\},\quad \text{if } U_a/\rho\ge k(1+s), \tag{4a}$$

$$\frac{d\rho}{dt}=B\left\{\frac{U_a}{\rho}-k(1-s)\right\},\quad \text{if } U_a/\rho\le k(1-s), \tag{4b}$$

$$\frac{d\rho}{dt}=0,\quad \text{if } U_a/\rho>k(1-s) \text{ and } U_a/\rho<k(1+s). \tag{4c}$$

A visualization of equation (4) is given in Figure 1.

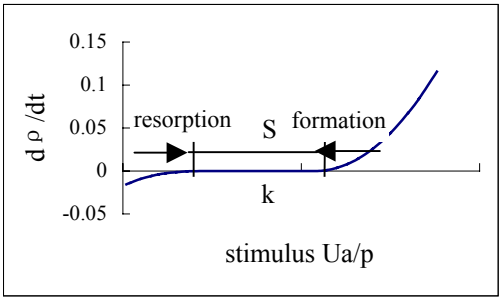

Figure 1. Relationship between density rate and stimulus

When the stimulus value is between k$\pm$sk, no bone remodeling will occur. If the stimulus value is outride this range, bone formulation or resorption takes place. According to the actual situation, for an equal value of the driving force U_a/ρ -k, the rate of density changes for resorption is larger than the rate of change in density change for formulation. Thus, Eq.(4) can be expressed as

$$\Delta\rho = B_1\left\{\frac{U_a}{\rho}-k(1\pm s)\right\}^{\alpha}\Delta t,\quad \text{if } U_a/\rho\ge k(1+s) \text{ or } U_a/\rho\le k(1-s), \tag{5}$$

where subscript α represents 2 or 3 respectively for formation or resorption. The boundary conditions for the predicted apparent densities is expressed as:

$$\rho_{\min} \le \rho \le \rho_{\max} . \tag{6}$$

In the present calculation, Eq.(6) is taken as $0.001 < \rho < 1.74 g/cm^3$, where $1.74 g/cm^3$ is the apparent density of the compact bone. A lower boundary of 0.001 (g/cm^3) instead of zero is taken, because zero density will lead to zero stiffness in the finite element analyses, which will give numerical problems. The relation between the elastic modulus and the bone density is taken as

$$E = K\rho^P \tag{7}$$

The value of p can be determined by the homogenization method computation of bone material elastic modulus. The constant k is often taken between 2000 and 3000.

2.2 Optimality-criterion algorithm

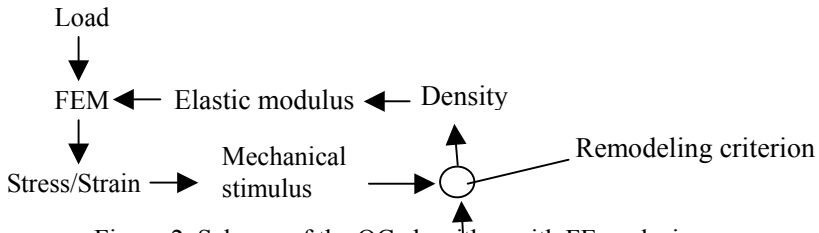

Figure 2. Scheme of the OC algorithm with FE analysis

A schematic representation of the computer simulation process is shown in Figure 2. The main procedures are as follows.

1. The values of stress, strain, and strain-energy density of structural elements of the bone are achieved by the finite element analyses.
2. Based on Eq.(5), we determine whether formation or resorption occurs, which is deduced by strain energy governing equations.
3. For the case of bone remodeling, the density or volume fraction ratio is changed. With the homogenization theory, the elastic modulus of bone can be calculated, and the iteration procedure returns to the finite element analysis of step 1.
4. If the mechanical stimulus does not induce bone remodeling, then the remodeling is finished. When remodeling is finished, it is assumed that the strain-energy density has distributed averagely or most of the bone elements have gotten their limits of the value of density. At that time, the computational process is finished.

The numerical simulation of bone remodeling can be achieved by solving the structural optimization problem via the iteration procedures above described. Based on the remodeling mechanism described in the strain-energy theory, the bone system induces, adjusts, responses, circulates, until the bone material distribution satisfy the optimization criterion of strain energy uniform distribution, which is the normal state of bone.

3 Computational Models of Bone Fracture Healing

To study the bone fracture healing process, the FE model of 4-node plane membrane is adopted. The elastic modulus is 187000 GPa and the value of Possion ratio is 0.3 (Zhang XQ et al, 2002). The middle part of the femur is selected for the present study, which is shown in Figure 3. Here, the outer parts of line a-b and c-d are virtual elements, and the inner parts of line a-b and c-d characterize the cross-section of the femur, which can be represented by different densities. The outer diameter of the bone is 26mm and the inner diameter is 10mm.

Using the initial state of the bone fracture healing process, we can outline the bone fracture healing process as the following four types: (1) type of osteotylus-absorbed. The case can be divided as follows: type of outer-osteotylus-absorbed, type of inner-osteotylus-absorbed, type of modulla cavity-jam-absorbed, type of severe-osteotylus-absorbed and type of inner-outer-osteotylus-absorbed. The density of the bone diaphysis is represented as ρ_1 and ρ_2, respectively. The value of ρ_1 is $1.7 g/cm^3$, and the value of ρ_2 is selected as $0.7 g/cm^3$ and $1.2 g/cm^3$. The five cases as shown in Figure 4 are simulated. (2) Type of osteoporosis. This case is shown in Figure 5. The density of bone diaphysis is lower than that of the normal bone diaphysis 1.7 g/cm^3. The cases of $\rho_1 = 1.2 g/cm^3$ and $\rho_1 = 0.7 g/cm^3$ are considered here. (3) Type of bone default-recovery. This type can be divided into three, which is expressed in Figure 6(a)(b)(c). The density of bone diaphysis is $1.7 g/cm^3$. The density of bone default part is represented as 0.1, 0.3 and 0.5(g/cm^3), respectively. The nine cases described above are simulated. (4) Type of synthesis, not discussed in this paper.

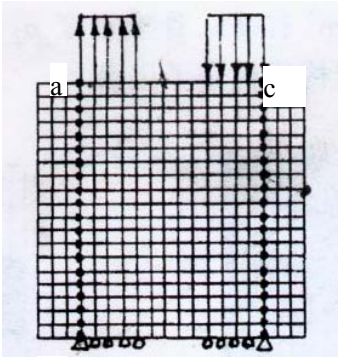

Figure 3. FEM model of a middle femur

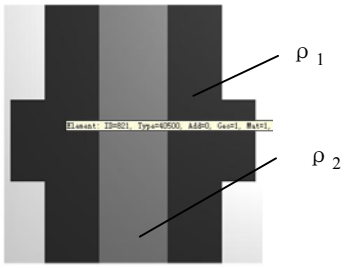

(a) Outer-osteotylus-absorbed

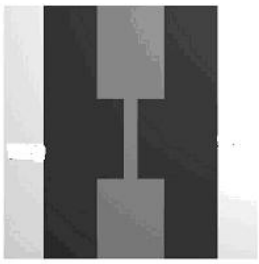

(b) Inner-osteotylus-absorbed

(c) Modulla cavity-jam-absorbed

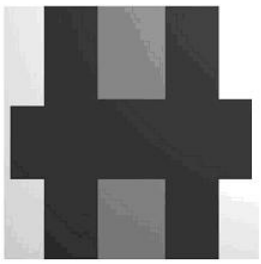

(d) Severe-osteotylus-absorbed

(e) Inner-outer-osteotylus-absorbed

Figure 4. Five types of osteotylus absorbed

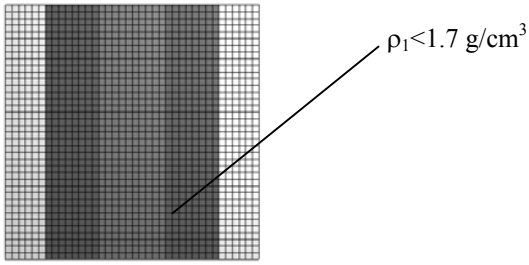

Figure 5. Type of osteoporosis

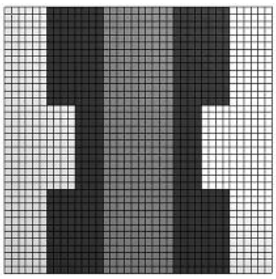

(a) Bone outer-default-recover

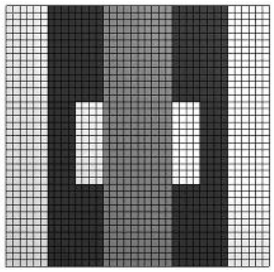

(b) Bone inner-default-recover

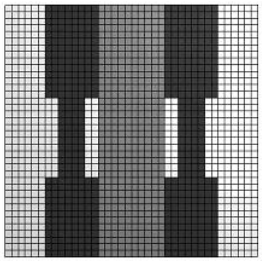

(c) Bone inner-outer-default-recover

Figure 6. Three types of bone default-recover

4 Numerical Simulation Results

In the following, the bone fracture healing process is predicted quantitatively, which can provide the mechanism of bone fracture healing. The type of osteotylus-absorbed, the type of osteoporosis recover and the type of default-recover of bone fracture healing plastic process are simulated here. It is to show the bone fracture healing plastic process results using strain energy density criterion.

4.1 Simulation of osteotylus-absorbed type healing

Two cases, (1) outer-osteotylus-absorbed type and (2) severe-osteotylus-absorbed, are shown in Figure 4. The simulation computational process of outer-osteotylus-absorbed type is shown in Figure 7. (a)-(f) is the healing process of time 0, 100, 150, 300, 350 and 500. The results show that the outer-osteotylus has been absorbed well.

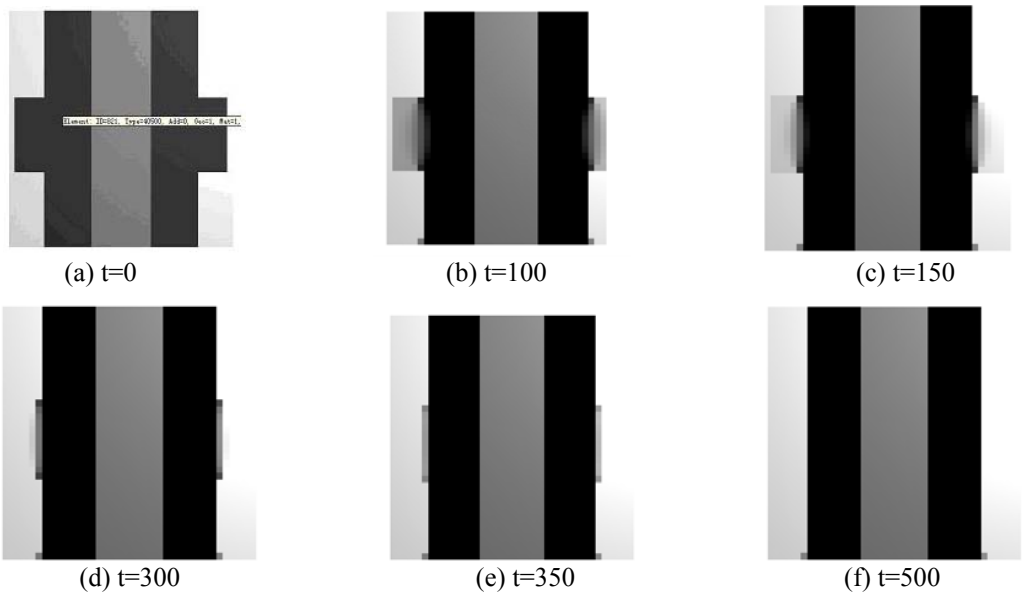

(a) t=0 (b) t=100 (c) t=150

(d) t=300 (e) t=350 (f) t=500

Figure 7. Plastic process of outer-osteotylus-absorbed

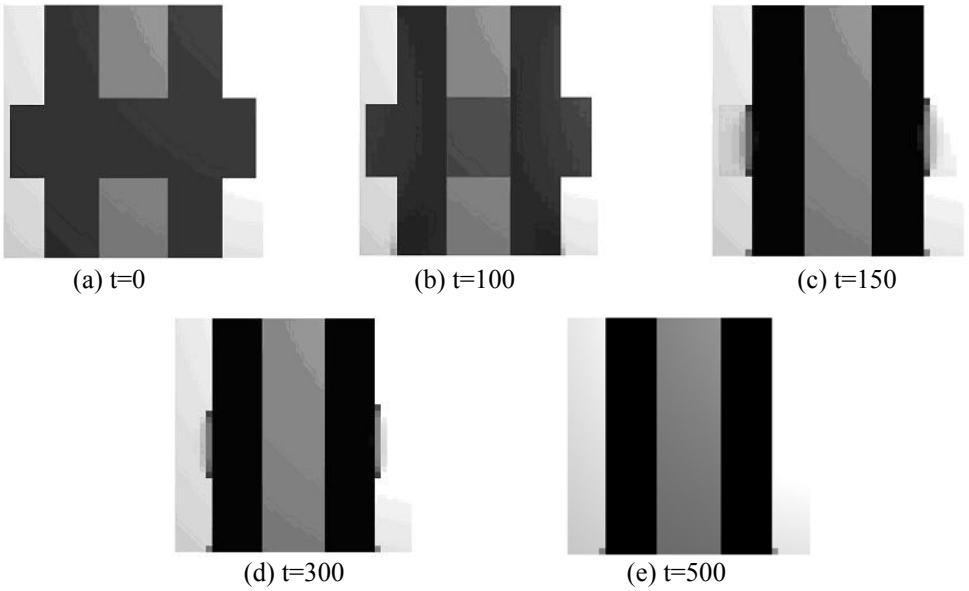

(a) t=0 (b) t=100 (c) t=150

(d) t=300 (e) t=500

Figure 8. Plastic process of severe-osteotylus-absorbed

The plastic process of severe-osteotylus-absorbed is shown in Figure 8. Similarly, the other three cases in Figure 4 are simulated here: inner-osteotylus-absorbed type, inner-outer-osteotylus-absorbed type and modulla cavity-jam-absorbed type. The results show that all the cases of osteotylus-absorbed type can reach their normal state. It can be concluded that for each type of osteotylus-absorbed, the osteotylus can be absorbed completely and the bone will recover its initial state.

We can analyze the results of Figure 7 and Figure 8. At the beginning of healing process, absorbing osteotylus is faster. With the time passing, the process of absorbing osteotylus is slower. It is seen in Figure 23. At first, the

density of bone osteotylus is 1.70g/cm^3. After healing process 100, the density of outer osteotylus falls to 0.8g/cm3 and the density of inner osteotylus is 1.2g/cm^3. After healing process 200, the density of outer osteotylus falls to 0.3g/cm^3 and the density of inner osteotylus is 1.0g/cm^3. After healing process 300, outer layer of outer-osteotylus almost fade away and inner layer of outer-osteotylus fade away slowly. Until the time is 500, the osteotylus will be disappeared completely.

In the following, as for three cases of bone fracture healing process, the relationship between the structural mass and the iteration are given in Figure 9. All the osteotylus, including outer-osteotylus, inner-osteotylus and any other type of osteotylus, can be absorbed in the bone remodeling and all the results have the identical mass even the initial osteotylus type is so different.

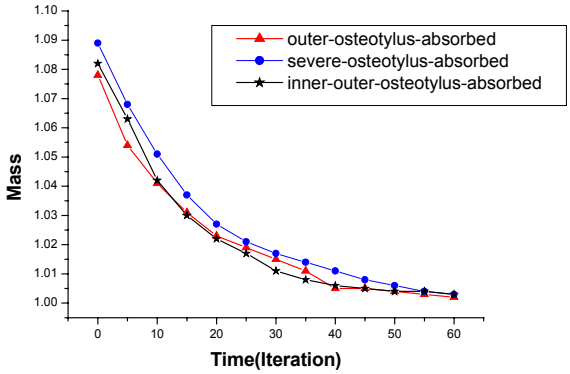

Figure 9. Relationship between bony mass and remodeling time

4.2 Simulation of osteoporosis type healing

The phenomenon of osteoporosis is very common in the clinic operation. The density of bone diaphysis is lower than that of the normal bone diaphysis shown in Figure 5. The phenomenon of osteoporosis is numerically simulated. The density of bone diaphysis is selected respectively 1.2g/cm^3 and 0.7g/cm^3.

The osteoporosis recover process is simulated by taking, for example, ρ_1=1,2g/cm^3. In each iteration, the time is updated by 10. The results of bone osteoporosis recover of time 0, 100, 200 and 300 are shown in Figure 10. The results show that although the thinner density in initial, the healing process can recover density to the normal state. The relationship between the bone diaphysis density, the bone mass and iteration (remodeling time) are given in Figure 11(a) and (b).

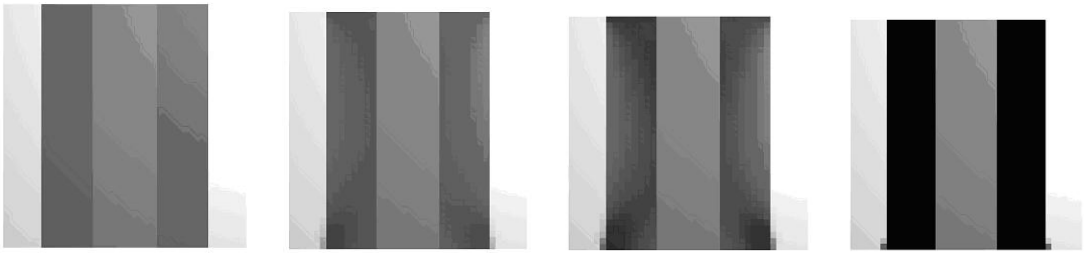

(a) t=0 (b) t=100 (c) N=20 (d) N=30

Figure 10. Plastic process of osteoporosis-recover

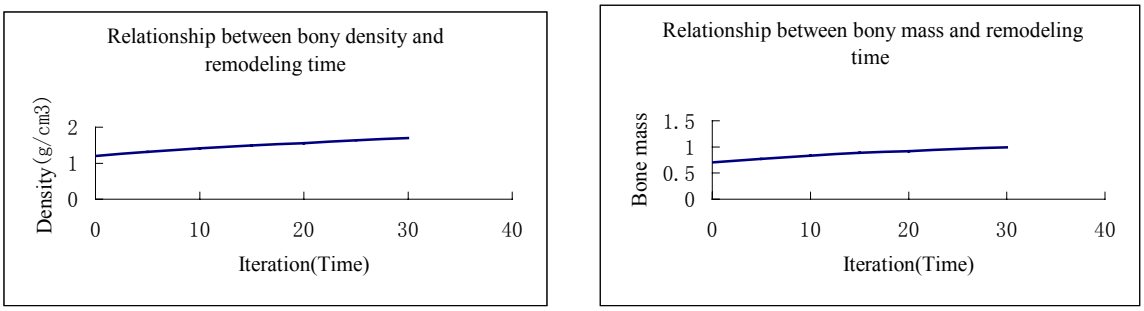

(a) Relationship between bony density and remodeling time

(b) Relationship between bony mass and remodeling time

Figure 11. Time dependent of osteoporosis-recover

4.3 Simulation of bone-default-recover

The case of bone-default is uncommon. Here, mainly a theoretical discussion is carried out to verify if the bone can recover the normal state after bone-default or not. Three kinds of bone-default cases are simulated, such as outer-default-recover, inner-default-recover and inner-outer-default-recover. The density of bone diaphasis ρ_1 is 1.7g/cm^3 and the density of bone-default ρ_3 is 0.1, 0.3 and 0.5(g/cm^3), respectively. The above 9 kinds of bone-default-recover process are simulated here. The type of bone outer-default-recover (ρ_3 = 0.1g/cm^3) and the type of bone inner-default-recover (ρ_3 = 0.1g/cm^3) are taken as the examples to illuminate the bone remodeling in detail. Figures 12 and 13 show the process of the above two cases.

From the results, it can be concluded:

1) The numerical simulation of each case of bone inner-outer-default-recover shows that the bone is not always able to recover completely. The total mass can only achieve 95% of the former.
2) Considering velocity of recovering, we deduce that the velocity is fast at the beginning of recover, and with passed time, the process of default-recover become more slowly. In the last phase of remodeling, the changing of total mass is very small.

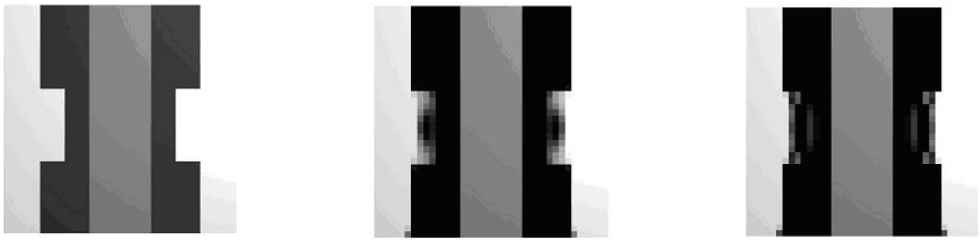

(a) t=0 (b) t=50 (c) t=100

(d) t=200 (e) t=300 (f) t=400

Figure 12. Plastic remodeling process of bone outer-default-recover

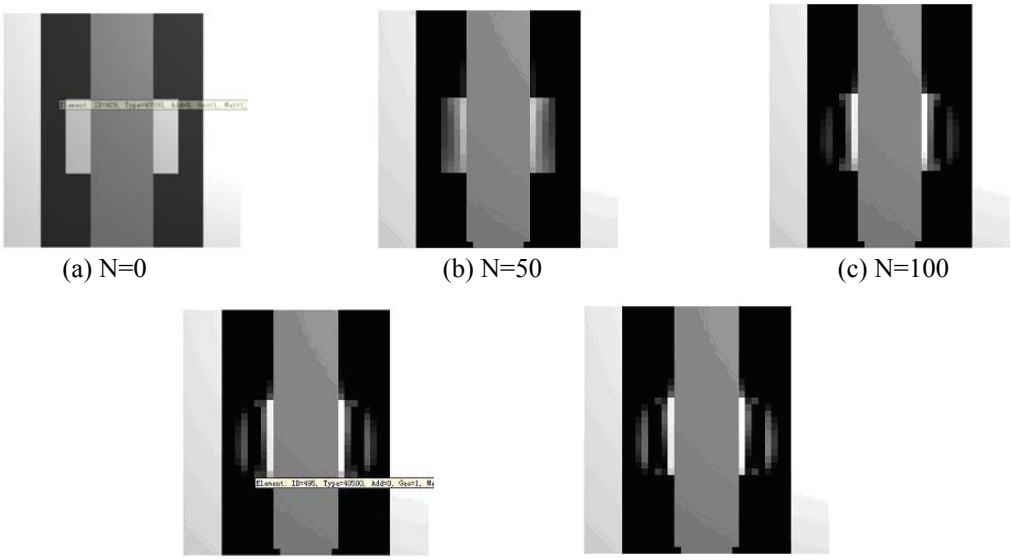

(a) N=0 (b) N=50 (c) N=100

(d) N=200 (e) N=300

Figure 13. Plastic remodeling process of bony inner-default-recover

5 Conclusions

In this paper, the strain-energy density criterion is applied to construct an optimization algorithm to simulate the internal remodeling of trabecular bones. The finite element method performs the numerical analysis of stress and strain of bones. From the results of remodeling simulation for three typical models, we draw the following

conclusions.

1) The results of numerical simulation is accordance with Wolff's law, i.e. the mechanical loading is the main factor driving bone remodeling, and the trabecular align with the directions of principal stress.
2) The strain-energy density criterion is effective to simulate the actual remodeling process of trabecular bones, which can reflect the characteristics of adaptive remodeling theory.
3) The simulation of the process of bone fracture healing gives good results. They are in accordance with the actual situation. It is also shown that the processing of bone fracture healing is the result of bone remodeling.

References

Fung Y.C. Biomechanics, The basic equication of biomechanics. University of California, San Diego, USA. 1990.

Fung Y.C. Biomechanics, Motion, Flow, Stress, and Growth. University of California, San Diego, USA. 1990.

Wloff J. Das Gesetz der. Transformation. der Knochen, Hirschwald, Berlin, 1892; 110-157.

Cowin S.C., Hegedus D.M. Bone remodeling: A theory of adaptive elasticity. J Elasticity, 1976; 6; 313-337.

Firoozbkhsh K, Cowin S.C. An analytical model of pauwels function adaptation mechanism for bone. ASME, J Biomech. Engin., 1981; 103; 246.

Currey J.D. The mechanical adaptations of bones. Princeton Univ. Press, 1984.

Fyhrie D.P., Carter D.R. A unifying principle relating stress to trabecular bone morphology. J. Biomech. 1986, 23, 1-10.

Fyhrie D.P., Schaffler M.B. The adaption of bone apparent density to applied load. J. Biomech. 1995, 28, 135-146.

Charles H.T., Vital A., Ramana M.V. A uniform strain criterion for trabecular bone adaption: do continuum-level strain gradients drive adaptation? J. Biomech. 1997, 30(6), 555-563.

Christopher R.J., Simo J.C., Beaupre G..S. Adaptive bone remodeling incorporating simultaneous density and anisotropy considerations. J. Biomech. 1997, 30(6), 603-613.

Carter D.R. Mechanical loading histories and skeletal biology, J. Biomech. 1987, 20, 785-794.

Stilpner M.A. Various continuum bone remodeling algorithms applied to the proximal femur in two and three dimensions, M. Sc. Thesis, Department of Mechanical Engineering, University of Cape Town

Huiskes R., Weinans H., Van Rietbergen B. The relationship between stress shielding and bone resorption around total hip stems and the effects of flexible materials. Clinical Orth. and Related Research, 1992, 274, 124-134.

Poss R., Robertson D., Walker P.S. and et al. Non-cemented total hip arthroplasty. Chap. 30: anatomic stem design for press-fit and cemented application, ed. R. Fitzgerald Jr. Raven Press, New York, 1988.

Angelo C., Marco V. and et al. Global asymptotic stability of bone remodeling theories: a new approach based on non-linear dynamical systems analysis. J. Biomechanics. 1998, 31, 289-294.

Martin L., Overgaard S. and et al. Transforming growth factor-β 1 adsorbed to tricalciumphosphate coated impants increases peri-implant bone remodeling. Biomaterial, 2001, 22, 189-193.

Treharne R.W. Review of Wolff's law and its proposed means of operation. Orthop Rev, 1981, 10, 35-47.

Weinbaum S, Cowin S.C., Zeng Y. A model for the excitation of osteocytes by mechanical loading-induced bone fluid shear stress. J. Biomechanics, 1994, 27, 339-360.

Zhu X.Y., Bai F.D., Dong X. and et al. Fumur face remodeling simulation after internal fixation with trihedral fix trough compression plate, Chinese Journal of Biomedical Engineering, 1997, 16(2), 128-133.

Zhang C.Q., Zhu X.Y., Mechanics in plastic stage of fracture union. Chinese Journal of Biomedical Engineering, 2002, 21(2), 132-137.